Наносистеми, наноматеріали, нанотехнології
Nanosistemi, Nanomateriali, Nanotehnologii
2025, т. 23, № 1, сс. 89–99
https://doi.org/10.15407/nnn.23.01.0089

PACS numbers: 61.05.cp, 78.20.Ci, 78.66.Li, 78.67.-n, 81.07.Bc, 81.15.Rs, 81.40.Tv

Study of the Structural and Optical Properties of Cu and Co Co-Doped ZnO Thin Films

Tayeb Saoud[1], Abdallah Diha[2], Said Benramache[1], and Amira Sbaihi[1]

[1]*Laboratoire des Matériaux,*
des Énergies et de l'Environnement,
University of Biskra,
07000 Biskra, Algeria
[2]*Mechanics Department,*
Tebessa University,
12000 Tebessa, Algeria

The Co and Cu co-doped thin ZnO films are successfully deposited on glass substrate by spray pneumatic method. In this work, it is obtained a semiconductor as Co and Cu co-doped thin ZnO films with good optical and electrical properties. XRD patterns of the Co and Cu co-doped thin ZnO films indicate that the obtained thin films are hexagonal ZnO (wurtzite, JCPDS 36-1451). Structural, optical, and electrical properties of thin films are studied as functions of atomic percentage (Co/Cu) co-doping thin ZnO films. It is fixed the doping level of atomic percentage of 2% Cu and various Co-doping atomic percentage (1.5%, 2%, 3%, 5%, 7%) in order to find out the influence of Co/Cu co-doping on thin ZnO film properties.

Тонкі плівки ZnO, леґовані Co і Cu, були успішно нанесені на скляну підкладинку пневматичним методом розпорошення. У даній роботі одержано напівпровідник у вигляді тонких плівок ZnO, леґованих Co і Cu, з хорошими оптичними й електричними властивостями. Рентґенограми тонких плівок ZnO, леґованих Co і Cu, вказують на те, що одержані тонкі плівки є гексагональним ZnO (вюрцит, JCPDS 36-1451). Структурні, оптичні й електричні властивості тонких плівок вивчено як функції атомового відсотка (Co/Cu)-леґування тонких плівок ZnO. Зафіксовано рівень атомового відсотка леґування у 2% Cu та різні атомові відсотки леґування Co (1,5%, 2%, 3%, 5%, 7%), щоб з'ясувати вплив на властивості тонкої плівки ZnO спільного (Co/Cu)-леґування.

Key words: ZnO, thin films, Co and Cu co-doping, spray pneumatic method.

Ключові слова: ZnO, тонкі плівки, леґування Co і Cu, розпорошувальний пневматичний метод.

(Received 21 October, 2023; in revised form, 20 April, 2024)

1. INTRODUCTION

ZnO is a natural semiconductor with a straight band gap of 3.37 eV and a huge exciton binding energy of 60 meV. It is one of the most important and increasingly popular semiconductor materials [1, 2]. ZnO has been widely employed in a variety of fields, including the automobile industry, medical equipment, communications, computers, spintronics, optoelectronics, biomaterials, data storage, energy conversion, and even architecture, due to its unique features [1–5].

It is crucial to figure out what element or elements ZnO has to be doped with in order to manage the band gap, electrical conductivity, and carrier concentration.

Because of the potential uses in spintronics, several researchers have recently focused on doping ZnO with transition metals (TMs) such as Mn, Ni, Fe, Cu, Co, and Cr [1–7].

Cu is virtually optimal for changing the characteristics of ZnO among the other doping elements because Cu atoms have a radius and electronic shell that are comparable to those of Zn atoms; consequently, replacing Zn with Cu does not result in a change in the lattice constant. Cu-doping effects on magnetism, photoluminescence, band gap, and transmittance of ZnO films generated by magnetron RF sputtering, magnetron DC sputtering, spray pyrolysis, pulsed laser deposition, and sol-gel methods have all been researched extensively [6–10].

This work seeks to obtain a semiconductor from Co and Cu co-doped ZnO thin films with good optical and electrical properties. We investigated the effect of different Co and Cu concentrations on the structural and optical properties of Co and Cu co-doped ZnO thin films. The ZnO thin films were deposited onto glass substrate by using the spray pneumatic method at 400°C for 2 ml/min of deposition rate.

2. MATERIALS AND METHODS

Prepared $Zn_{1-(0.02+y)}Cu_{0.02}Co_yO$ thin films were deposited by using the spray pyrolysis technique onto glass substrates. The solution was prepared by dissolving zinc acetate ($Zn(CH_3CO_2)_2$, $2H_2O$) in distilled water to a 0.1 M solution, with cobalt chloride ($CoCl_2$, $6H_2O$) and copper nitrate ($Cu(NO_3)_2$, $3H_2O$). The atomic percentage of [Co–Cu] was varied as 1.5%, 2%, 3%, 5%, and 7 at.%. The solution was sprayed onto the preheated substrates at and held at optimized sub-

strate temperature (380°C) substrate temperature, the distance between the nozzle and substrates (25 cm) was kept constant for all experiments.

The structural characterization of deposited thin films was carried out by analysing the x-ray diffraction patterns recorded by (XRD, Bruker AXS-8D) with ($\lambda_{\mathrm{Cu}K_\alpha} = 0.15406$ nm) by varying the scanning range of (2θ) from 20° and 90°. The ultraviolet visible spectrophotometer (JASCO V-770 UV-Vis/NIR)) to find the transmittance, band gap and Urbach energy.

2. RESULTS AND DISCUSSION

2.1. Structural Properties

To determine the structure of Co and Cu co-doped ZnO thin films, spray pyrolysis samples were deposited on glass substrates at atomic percentage of Cu was 2 at.% and Co was varied as 1.5, 2, 3, 5 and 7 at.%. The films' XRD patterns were captured using a diffractometer and CuK_α. Source of radiation (with wavelength = 1.506 nm). The XRD scan was performed on a scale of 20° to 90°. The XRD diffraction patterns of Co and Cu co-doped ZnO thin films deposited at different atomic percentage of Cu using the spray pyrolysis technique are shown in Fig. 1.

In all the Co and Cu co-doped ZnO thin films, XRD diffraction peaks from the (100), (002), and (101) planes were found. For all the samples, the observations revealed three diffraction peaks, the greatest at 2θ = 31.6°, 2θ = 34.4° and 36.1°, matching to the following plans (100), (002) and (101), respectively. This indicates that Co

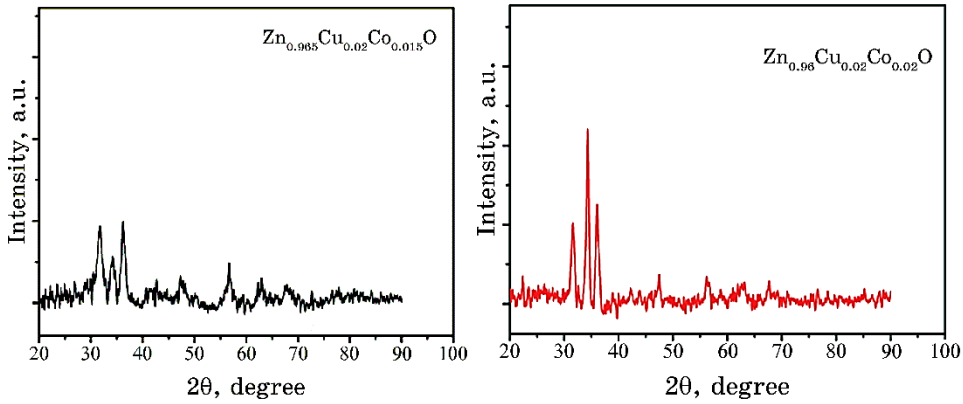

Fig. 1. X-ray diffraction spectra of fabricated $Zn_{0.965}Cu_{0.02}Co_{0.015}O$ thin films.

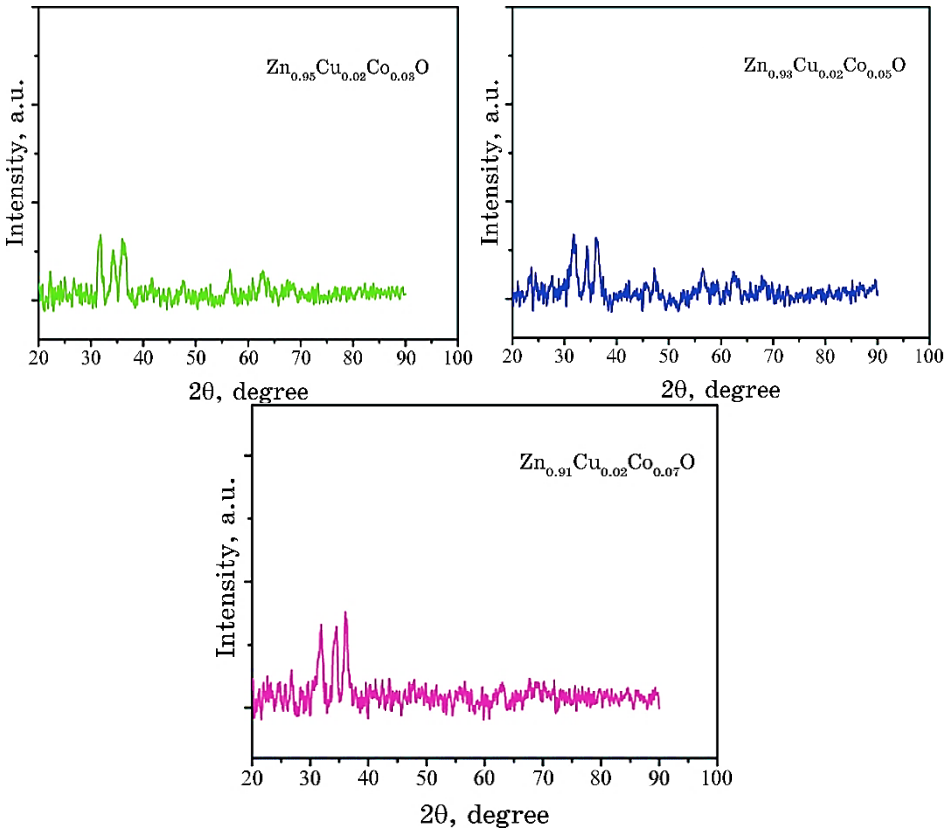

Continuation **Fig. 1.**

and Cu co-doping have no effect on the structure of ZnO. There are no additional peaks (such as Co, CoO, Cu, CuO, Cu_2O). Furthermore, with the Cu ions doping, all of the diffractive peaks in the XRD patterns gradually shift to the lower angle side [11].

The lattice constants a for <100> plane and c for <002> plane are computed from Refs. [12, 13]:

$$\frac{1}{d_{hkl}^2} = \frac{4}{3}\left(\frac{h^2 + hk + k^2}{a^2}\right) + \frac{l^2}{c^2}. \tag{1}$$

The average crystallite sizes determined in Table 1 were calculated from following relation:

$$D_m = \frac{D_{100} + D_{002} + D_{101} + D_{102}}{4}, \tag{2}$$

where β_{hkl} is the $FWHM$, K is a constant equal to 0.90, λ is the

TABLE 1. Lattice parameters, average crystallite size D_m and mean strain ε in $Zn_{0.98}Cu_{0.02}Co_xO$ thin films

Sample name	a, Å	c, Å	Average crystallite size D_m, nm	Mean strain ε, %
ZnO	3.260	5.223	35.607	0.33
$Zn_{0.965}Cu_{0.02}Co_{0.015}O$	3.253	5.250	27.701	0.85
$Zn_{0.96}Co_{0.02}Cu_{0.02}O$	3.274	5.226	29.760	0.38
$Zn_{0.95}Cu_{0.02}Co_{0.03}O$	3.2484	5.239	25.697	0.63
$Zn_{0.93}Cu_{0.02}Co_{0.05}O$	3.380	5.214	23.376	0.15
$Zn_{0.91}Cu_{0.02}Co_{0.07}O$	3.249	5.233	33.074	0.52

wavelength of the incident x-rays ($\lambda = 0.15406$ nm), D is the crystallite size, and θ is the Bragg angle.

The mean strain ε in the films in the direction of the c-axis calculated from the following relation:

$$\varepsilon = \frac{C_{\text{film}} - C_0}{C_0} \cdot 100\%, \tag{3}$$

where $C_0 = 5.206$ Å.

It can observed the average crystallite size D_m increase when Co (at.%) = 1.5% to 2% and decrease with Co (at.%) = 3% to 5%, then, increase Co (at.%) = 7%.

It can be seen the change in cell parameters caused by (Cu, Co) co-doped ZnO thin film.

The texture coefficient (TC_{hkl}), in terms of each directional intensity (I_{hkl}) is calculated to the corresponding intensity of the JCPDS card (I_{0hkl}). From it, we take information about the growth potential according to the trend [hkl].

The parameter (TC_{hkl}) is given by the following relationship [14]:

$$TC_{hkl} = \frac{\frac{I_{hkl}}{I_{0hkl}}}{\frac{1}{N}\sum_{i=1}^{n}\frac{I_{hkl}}{I_{0hkl}}}, \tag{4}$$

where N is the number of diffraction peaks.

The texture modulus values for the peaks of thin films of ZnO and $Zn_{0.98-y}Co_{0.02}Cu_yO$ are shown in Fig. 2.

It should be noted, the value of the largest texture coefficient for all films corresponds to the peak (002), indicating that it is the preferred orientation except for the film $Zn_{0.965}Cu_{0.02}Co_{0.015}O$ whose orientation was according to the peak (100).

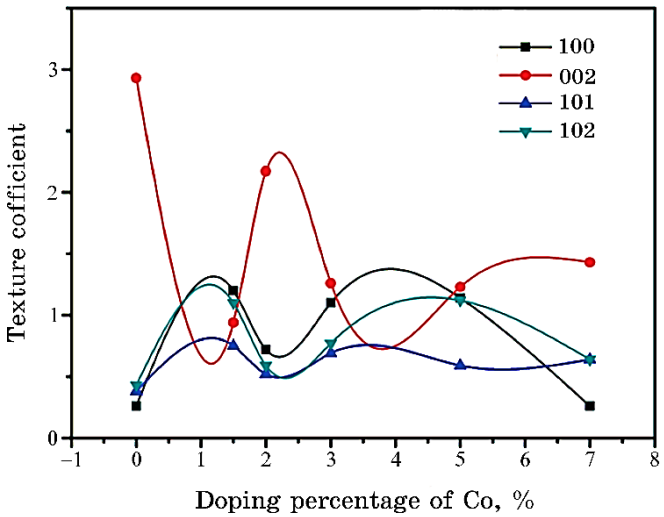

Fig. 2. Texture coefficient values for all peaks of fabricated ZnO and $Zn_{0.98-x}Cu_{0.02}Co_xO$ thin films.

2.2. Optical Properties

In the wavelength range from over 300 nm to 1200 nm, optical transmittance and absorbance *versus* wavelength curves of the Co and Cu co-doped ZnO deposited onto glass substrates at different atomic percentage of Cu were measured. Thin film transmittance and absorbance are depicted in Figs. 3 and 4, where the highest transmittance values are around 95%. The transmittance initially decreases with Co (= 2 at.%), then, increase, but with fewer fringes.

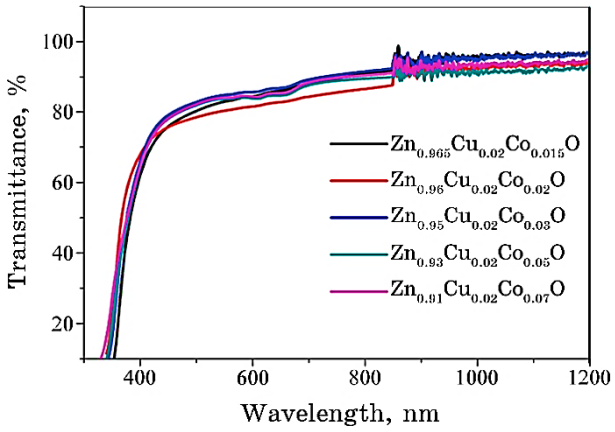

Fig. 3. Transmission spectra of fabricated $Zn_{0.98-x}Cu_{0.02}Co_xO$ thin films.

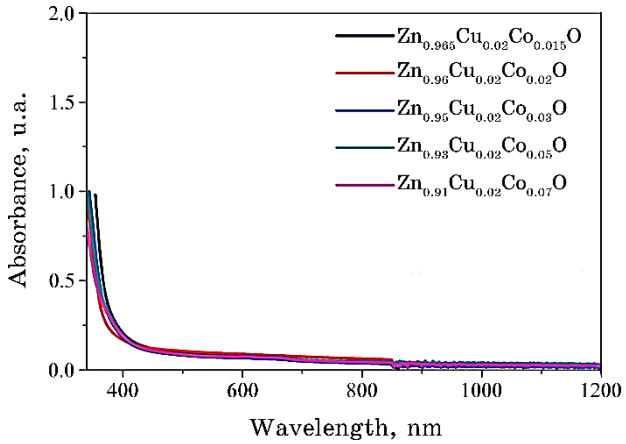

Fig. 4. Absorbance spectra of fabricated $Zn_{0.98-x}Cu_{0.02}Co_xO$ thin films.

It should be noted that the optical transmission spectra recorded in the visible region are related to electronic transitions and help to understand the electronic band structure of semiconducting films [15, 16].

The absorption edge corresponds to the electronic excitation of the valence band at the conduction band, which determines the direct optical band gap value. The well-known equation [17] connects incident photon energy $h\nu$ and absorption coefficient α. Thin films' direct optical band-gap values are calculated by extrapolating the straight-line portion of the $(\alpha h\nu)^2 = f(h\nu)$ (Fig. 5). By drawing $\ln\alpha$ *versus* $h\nu$, we can determine E_u value as the reciprocal of the linear part slope graph in Fig. 6. The direct optical band gap and the Urbach energy values of thin films are shown in Table 2.

The variation of optical band gap E_g and Urbach energy E_u of fabricated $Zn_{0.98-x}Cu_{0.02}Co_xO$ thin films *versus* Co (at.%) shown in Fig. 7.

The structural, optical and electrical properties of Co and Cu co-doped ZnO thin films were studied. Samples were deposited from Co and Cu co-doped ZnO thin films using the pneumatic spray technique, where, in the first samples $Zn_{0.98-y}Co_{0.02}Cu_yO$, we fixed the percentage of Co at 2% and varied the percentage of Cu at 1.5, 2, 3.5 and 7%, and in the second samples $Zn_{0.98-x}Cu_{0.02}Co_xO$, we fixed the percentage of Cu at 2% and varied the percentage of Co at 1.5, 2, 3.5 and 7%. The crystal sizes of all samples were estimated using Scherer's equation and were in the nanometer range. The optical properties of the samples were determined by ultraviolet visible spectrophotometer. The average crystal size was between 14.668 and 31.820 nm for $Zn_{0.98-y}Co_{0.02}Cu_yO$ and between 23.376 and 33.074 nm for $Zn_{0.98-x}Cu_{0.02}Co_xO$. The average crystal size for $Zn_{0.98-y}Co_{0.02}Cu_yO$

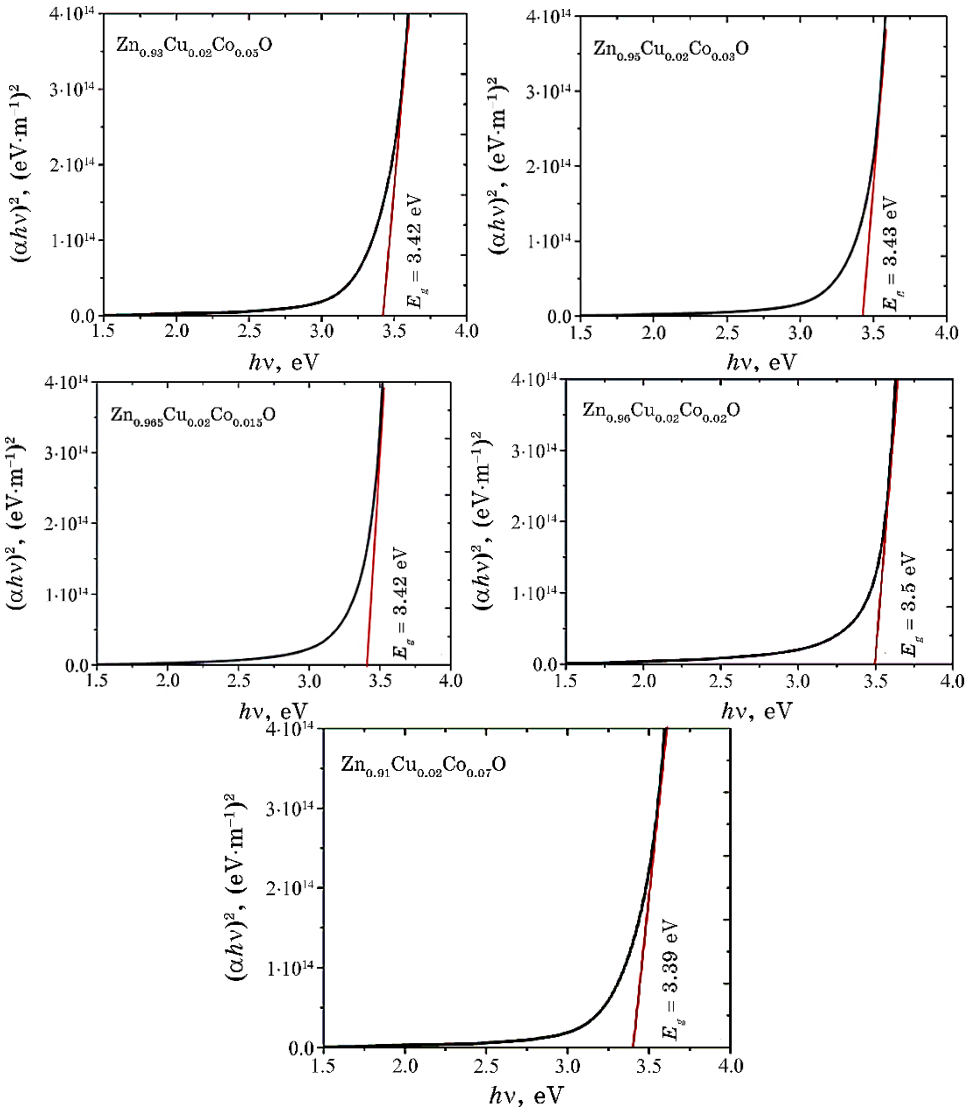

Fig. 5. $(\alpha h\nu)^2$ *versus* $h\nu$ for fabricated $Zn_{0.98-x}Cu_{0.02}Co_xO$ thin films.

samples was slightly smaller than the average crystal size for $Zn_{0.98-x}Cu_{0.02}Co_xO$. The band gap energy of $Zn_{0.98-y}Co_{0.02}Cu_yO$ samples was between 3.31 and 3.50 eV. The band gap energy of the $Zn_{0.98-x}Cu_{0.02}Co_xO$ samples is between 3.39 and 3.50 eV. The band gap energy of $Zn_{0.98-y}Co_{0.02}Cu_yO$ samples was slightly smaller than the band gap energy of $Zn_{0.98-x}Cu_{0.02}Co_xO$ samples.

Comparisons of two $Zn_{0.965}Co_{0.02}Cu_{0.015}O$ and $Zn_{0.93}Co_{0.02}Cu_{0.05}O$

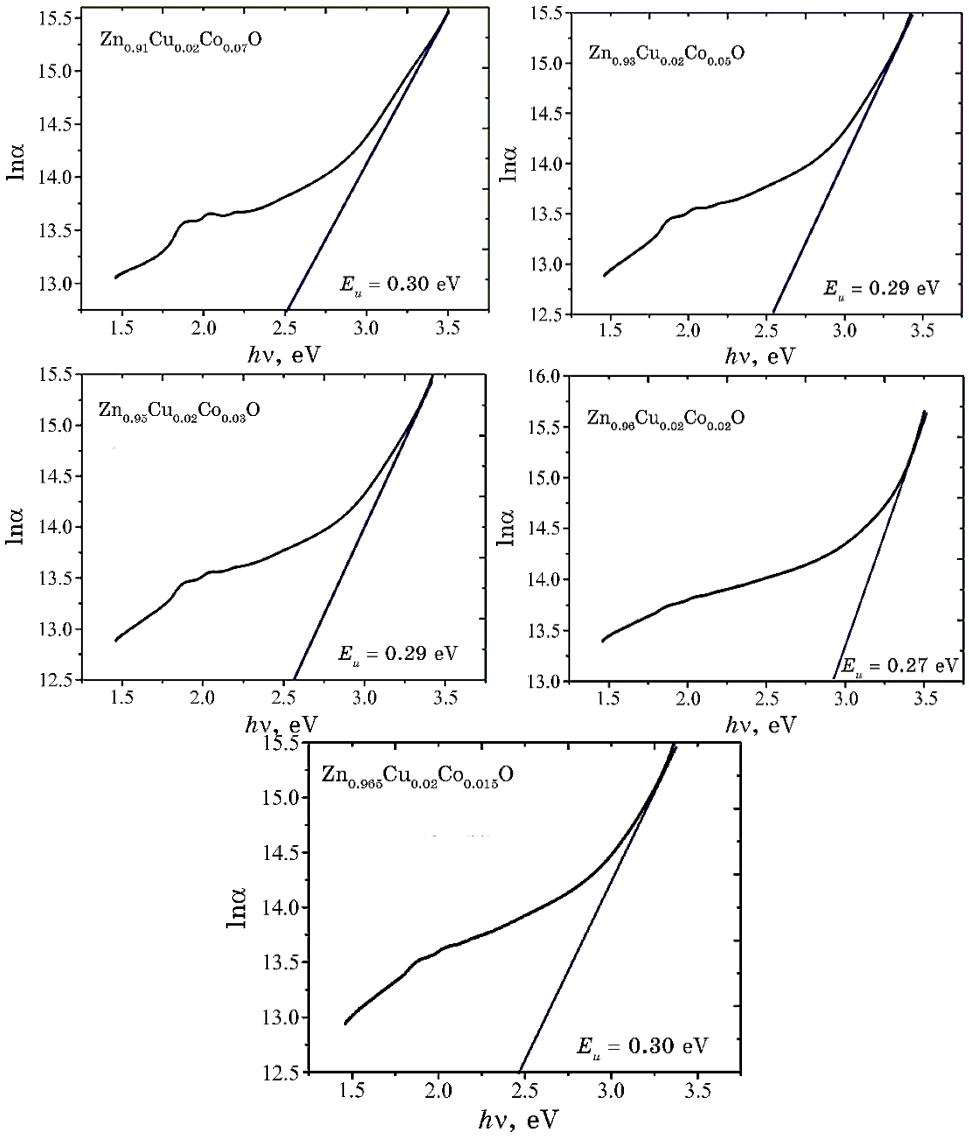

Fig. 6. lnα *versus* $h\nu$ for fabricated $Zn_{0.98-x}Cu_{0.02}Co_xO$ thin films.

samples with two samples $Zn_{0965}Cu_{0.02}Co_{0.015}O$ and $Zn_{0.91}Cu_{0.02}Co_{0.07}O$ that have less D_m and less E_g are shown in Table 3.

3. CONCLUSION

In this work, we investigated the effect of atomic doping ratio on

TABLE 2. Band gap energy E_g and Urbach energy E_u.

Sample name	E_g, eV	E_u, eV
$Zn_{0965}Cu_{0.02}Co_{0.015}O$	3.40	0.30
$Zn_{0.94}Cu_{0.02}Co_{0.02}O$	3.50	0.27
$Zn_{0.95}Cu_{0.02}Co_{0.03}O$	3.43	0.29
$Zn_{0.93}Cu_{0.02}Co_{0.05}O$	3.42	0.29
$Zn_{0.91}Cu_{0.02}Co_{0.07}O$	3.39	0.30

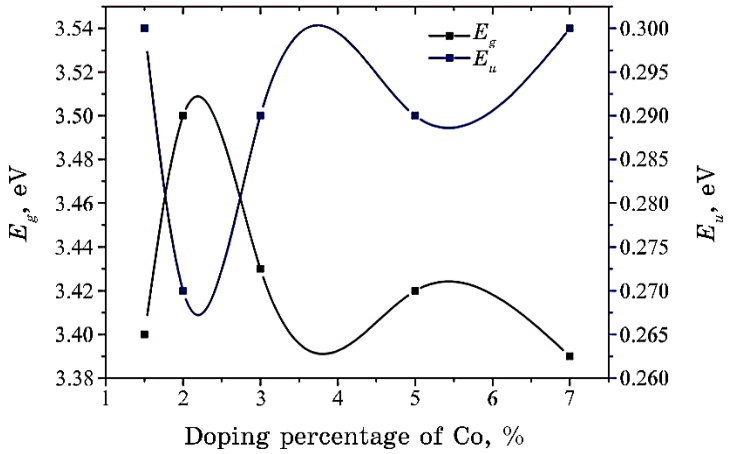

Fig. 7. The variation of optical band gap E_g and Urbach energy E_u of fabricated $Zn_{0.98-x}Cu_{0.02}Co_xO$ thin films *versus* Co (at.%).

TABLE 3. Comparison of structural and optical properties.

Sample	Average crystallite size D_m, nm	ε, %	E_g, eV	E_u, eV	σ, s/m
$Zn_{0.965}Co_{0.02}Cu_{0.015}O$	31.820	0.30	3.35	0.31	
$Zn_{0.93}Co_{0.02}Cu_{0.05}O$	27.4222	0.21	3.31	0.33	
$Zn_{0965}Cu_{0.02}Co_{0.015}O$	27.701	0.85	3.40	0.30	
$Zn_{0.91}Cu_{0.02}Co_{0.07}O$	33.074	0.52	3.39	0.30	

optical properties.

The structural and electrical properties of films deposited by spray pyrolysis technique were investigated. The XRD results showed that the precipitated films are single-phase and polycrystalline, and have a hexagonal structure with high-density peaks along the [002] direction, except for the film $Zn_{0.965}Cu_{0.02}Co_{0.015}O$ has a high peak along the direction (100). The average crystal size D_m was

found to be increasing with Co (at.%) = 1.5% to 2% and decreasing with Co (at.%) = 3% to 5%, then, increasing with Co (at.%) = 7%. Optical properties analysis showed that the direct optical band gap values of the fabricated thin films are varied from 3.39 eV to 3.5 eV.

REFERENCES

1. E. Asikuzun, O. Ozturk, L. Arda, and C. Terzioglu, *J. Molec. Struct.*, **1165**: 1 (2018); https://doi.org/10.1016/j.molstruc.2018.03.053
2. Y. Aoun, M. Marrakchi, S. Benramache, B. Benhaoua, S. Lakel, and A. Cheraf, *Mater. Res.*, **21**: e20170681 (2018); https://doi.org/10.1590/1980-5373-MR-2017-0681
3. Y. Ammaih, A. Abderrazak, B. Hartiti, A. Ridah, P. Thevenin, and M. Siadat, *Opt. Quant. Electro.*, **46**: 229 (2014); https://doi.org/10.1007/s11082-013-9757-2
4. Z. K. Heiba and L. Arda, *J. Molec. Struct.*, **1022**: 167 (2012); https://doi.org/10.1016/j.molstruc.2012.04.091
5. S. Benramache, *Annals of West University of Timisoara - Physics*, **61**: 64 (2019); https://doi.org/10.2478/awutp-2019-0006
6. S. Benramache, F. Chabane, and A. Arif, *Materials and Geoenvironment*, **67**: 35 (2020); https://doi.org/10.2478/rmzmag-2020-0001
7. E. Asikuzun, O. Ozturk, and L. Arda, *J. Mater. Sci.: Mater. Electron.*, **28**: 14314 (2017); https://doi.org/10.1007/s10854-017-7291-x
8. A. Guler, L. Arda, N. Dogan, and C. E. Boyraz, *Ceram. Int.*, **45**: 1737 (2019); https://doi.org/10.1016/j.ceramint.2018.10.056
9. C. Boyraz, N. Dogan, and L. Arda, *Ceram. Int.*, **43**: 15989 (2017); https://doi.org/10.1016/j.ceramint.2017.08.184
10. A. Diha, S. Benramache, and L. Fellah, *J. Nano- Electron. Phys.*, **11**: 03002 (2019); https://doi.org/10.21272/jnep.11(3).03002
11. P. Cao and Y. Bai, *Adv. Mater. Res.*, **774–776**: 964 (2013); https://doi.org/10.4028/www.scientific.net/AMR.774-776.964
12. C. Boyraz, N. Dogan, and L. Arda, *Ceram. Int.*, **43**: 15986 (2017); https://doi.org/10.1016/j.ceramint.2017.08.184
13. A. Javadian and M. R. Fadavieslam, *J. Mater. Sci.: Mater. Electron.*, **33**: 23362 (2022); https://doi.org/10.1007/s10854-022-09098-5
14. H. Hakkoum, A. Moumen, M. Ghougali, N. Sengouga, and E. Comini, *J. Mater. Sci.: Mater. Electron.*, **33**: 26604 (2022); https://doi.org/10.1007/s10854-022-09336-w
15. S. Abed, H. Bougharraf, K. Bouchouit, Z. Sofiani, B. Derkowska-Zielinska, M. S. Aida, and B. Sahraoui, *Superlatt. Microstruct.*, **85**: 370 (2015); https://doi.org/10.1016/j.spmi.2015.06.008
16. D. Miao, H. Hu, and L. Gan, *J. Alloys Compounds*, **639**: 400 (2015); https://doi.org/10.1016/j.jallcom.2015.03.189
17. S. Benramache, Y. Aoun, R. Gacema, and H. Mourghad, *Nanosistemi, Nanomateriali, Nanotehnologii*, **19**, Iss. 1: 147 (2021); https://doi.org/10.15407/nnn.19.01.147